Inferring the thermal resistance and effective thermal mass of a wall using frequent temperature and heat flux measurements

CrossMark

Phillip Biddulph [a],[*], Virginia Gori [a], Clifford A. Elwell [a], Cameron Scott [b], Caroline Rye [b], Robert Lowe [a], Tadj Oreszczyn [a]

[a] UCL Energy Institute, 14 Upper Woburn Place, London WC1H 0NN, UK
[b] Archimetrics Ltd seconded to the Complex Built Environment Systems Group (CBES), The Bartlett School of Graduate Studies, UCL, 14 Upper Woburn Place, London WC1H 0NN, UK

ARTICLE INFO

ABSTRACT

Evaluating how much heat is lost through external walls is a key requirement for building energy simulators and is necessary for quality assurance and successful decision making in policy making and building design, construction and refurbishment. Heat loss can be estimated using the temperature differences between the inside and outside air and an estimate of the thermal transmittance (U-value) of the wall. Unfortunately the actual U-value may be different from those values obtained using assumptions about the materials, their properties and the structure of the wall after a cursory visual inspection.

In-situ monitoring using thermometers and heat flux plates enables more accurate characterisation of the thermal properties of walls in their context. However, standard practices require that the measurements are carried out in winter over a two-week period to significantly reduce the dynamic effects of the wall's thermal mass from the data.

A novel combination of a lumped thermal mass model, together with Bayesian statistical analysis is presented to derive estimates of the U-value and effective thermal mass. The method needs only a few days of measurements, provides an estimate of the effective thermal mass and could potentially be used in summer.

© 2014 The Authors. Published by Elsevier B.V. This is an open access article under the CC BY license (http://creativecommons.org/licenses/by/3.0/).

1. Introduction

Energy use in buildings accounts for approximately a third of global primary energy consumption [1], half of which is used for space heating and cooling and hot water production. Ambitious CO_2 reduction targets have been agreed internationally to mitigate climate change [2,3], such as the UK's commitment to reduce emissions by 80% from 1990 levels by 2050 [4]. Reducing emissions from the built environment will be an essential component of these strategies; forecasts show that the energy demand associated with building use may grow [1], but that aggressive policy actions could potentially reduce the energy needs for space heating and cooling by approximately 47%. Numerous models and software tools have been developed to simulate the performance and energy demand of the built environment [5]. Such simulations are used by policy makers to inform large-scale long-term strategies to cut energy consumption in the built environment [6], or by professionals to

assess the energy performance of dwellings [7–9], and evaluate the cost-effectiveness of energy-saving measures during retrofitting or building design. However, some studies have revealed a lower than expected improvement in energy performance of the building envelope following retrofitting energy saving measures [10,11], with significant impact on the cost effectiveness of intervention.

The energy performance of the building envelope may be accurately estimated for well-characterised systems [10,12]. For walls, the required parameters include the thickness and in-situ thermal performance of their constituent layers, whilst inaccuracies in these quantities (e.g., thermal resistance and thermal mass) are a major source of uncertainty in the energy performance simulations [12]. However, accurate identification of appropriate thermal properties and thicknesses can be challenging for existing and new walls [12]. Tabulated values of thermal resistance and mass from the literature or software libraries are generally used, plus estimated thicknesses of the expected wall layers, following visual inspection. Significant inaccuracies can result from simulation outputs utilising published thermal values, as the range of thermal properties for visually similar materials can be large [13], for example the thermal conductivity of concrete ranges from 0.76 to 1.37 W m^{-1} K^{-1} [14]. Similarly,

* Corresponding author. Tel.: +44 20 3108 5908.
E-mail address: p.biddulph@ucl.ac.uk (P. Biddulph).

Nomenclature

R, R_1, R_2 Thermal resistance or R-Value, $m^2\,K\,W^{-1}$

U-Value Thermal transmittance ($=1/R_{Total}$), $W\,m^{-2}\,K^{-1}$

$T_{mass}, T_{int}, T_{ext}$ Temperature of the thermal mass, of the air near the interior and exterior of the surface of the wall respectively, $^{\circ}C$

Q Heat flow into the internal surface of the wall, $W\,m^{-2}$

C Effective thermal mass of the wall, $J\,m^{-2}\,K^{-1}$

τ Time step duration between successive recordings, s

p Time step index number. Data recording index. -

$P()$ Probability distribution. -

H_i, D, I Hypothesis (the ith hypothesis), Data and background Information. -

$stat, sys\text{-}W, sys\text{-}inst, sys+stat$ Indicates that the error is statistical; systematic due to wind and moisture; systematic due to instrumentation; systematic combined with statistical. -

$\sigma_{W+TM}, \sigma_W, \sigma_{TM}$ Uncertainty in the U-value due to wind, moisture and thermal mass; due to wind and moisture only; due to thermal mass only, $W\,m^{-2}\,K^{-1}$

estimating the internal structure of a wall by visual inspection, or from assumptions of the construction, introduces potentially significant error into energy performance estimates [15]. In addition to error in estimating the thickness of layers and their variability across a wall, uncertainties include inhomogeneities in the structure such as thermal bridges, gaps in the materials and delamination, air movement in cavities, moisture content, and local and seasonal environmental conditions [15–18].

Many errors associated with estimating thermal performance from published values and assumptions of wall structure may be avoided by utilising in-situ measurements to estimate the actual thermal properties of building elements. In-situ estimates of thermal performance may also form part of construction quality assurance procedures [15]. The measurement of heat flux and nearby air or surface temperatures can be used to estimate the effective thermal mass, thermal resistance (R-value), or equivalently, thermal transmittance (U-value) [19] of walls. The combination of the effective thermal mass, as opposed to the total thermal mass, and the thermal resistance is analogous to the complex internal thermal admittance as used in frequency domain analysis of walls [20]. Such techniques account for uncertainty in the thermal properties of elements of the wall, their thickness and state of conservation [15], but not of inhomogeneities in the wall construction.

The estimation of thermodynamic parameters (i.e. R-value and thermal mass) of real building elements from the analysis of in-situ measurements is not commonplace, but in recent years considerable interest has been shown in such in-situ performance characterisation [13,15,16,21]. However, steady-state methods [22] are time consuming, seasonally bounded [23] and aim to eliminate the effect of thermal mass, rather than characterise it; dynamic methods may be used to provide more insight into building performance, and may be applied in a wider range of conditions. Studies have been carried out in outdoor test cells to inform in-situ dynamic techniques through the PASSYS project and the PASLINK Network by investigating the thermal performance of well-known building components under real dynamic conditions [24]. These projects have improved testing procedures and the development of dynamic analysis methods for thermodynamic parameter prediction.

In this paper we propose a novel combination of a simple lumped thermal mass model and Bayesian analysis that provides the opportunity for the wider use of real data to assess the performance of buildings in their environment and the impact of interventions. The use of lumped capacitance models to infer thermodynamic properties of building elements is not new in the field [25,26]. However, the proposed analysis technique provides some advantages. Firstly, a significantly shorter measurement campaign may be possible in many conditions. Secondly, because Bayesian analysis is used throughout, the statistical evidence for different models of heat flow may be compared. The method also provides estimates of statistical uncertainties for the inferred parameters and accounts for relationships between them. Thirdly, it enables simultaneous characterisation of the effective thermal mass and the R-value of the element, which is not possible with conventional steady-state methods. Finally, the presented method utilises a simple model of the wall using only four unknown parameters, without the need for additional assumptions on the component's structure and performance, unlike many more complicated dynamic models [25,26]. These parameters may be fully characterised with the typically recorded time series of internal and external temperatures, plus heat flux on the inside face of the building component.

2. Case study and monitoring campaign

The dataset analysed in this paper was collected during the winter of 2010 by the Building Services Research and Information Association (BSRIA) as part of a study to investigate the U-values of walls in occupied domestic properties [21]. Walls at 93 different sites across England were monitored and were expected to be solid (with no cavity or insulation). Measurements were collected in accordance with ISO 9869:1994 [21,22]. Sensors were ideally placed on north-facing walls to exclude the impact of solar radiation on the external surface and away from internal sources of heat [21]. Moreover, sensors were usually placed with reference to structural features; however, sensor location was compromised in some cases for the convenience of the occupants [21]. The wall was instrumented with a heat flux meter (HFM) and thermistor temperature sensors [22]; the data were averaged over 5 minutes and recorded by Eltek 401 [27] data loggers. The HFM (Hukseflux HFP01 [28]) was placed on the inside surface of the wall. Silicon grease was used to achieve good thermal contact between the HFM and the wall surface, while a thin PVC film was applied to protect the wall surface. The thermistors were placed in the air near the internal and external surfaces of the wall. Internally the temperature sensor was placed as close as possible to the HFM. Surface mounted thermometers are often used to minimise deviations due to air movements and wind [29]. However, fixed estimates of the boundary layer resistances must then be incorporated into U-value calculation. Appropriately placed air temperature thermometers can be used to account for real environmental conditions adjacent to the wall and better reflect the real in-situ U-values.

The data presented in this paper comes from a single wall in a terraced house, which was typical of all the walls surveyed, it was approximately 300 mm thick and of brick construction. Measurements of the heat flux, Q, (Fig. 4) and air temperatures, T_{int} and T_{ext}, (Fig. 5) were made over a 14-day period in February 2010.

3. Theory and calculation

3.1. Conventional methods

3.1.1. Calculating the thermal properties using assumed material properties

Physical measurements of the individual components of the wall were not made during the survey, however a rough identification

of the bulk material (brick) and thickness (300 mm) of the wall was established. The likely range of R-values for the wall may be estimated, assuming [14]:

- the brick is solid and the thermal conductivity lies in a typical range in the literature: from 0.69 to 1.32 W m^{-1} K^{-1};
- there is a thin layer (10 mm) of plaster (gypsum) with a thermal conductivity of 0.48 W m^{-1} K^{-1} on the inner surface of the wall;
- the internal surface resistance is 0.13 W^{-1} m^2 K;
- and the external surface resistance is 0.04 W^{-1} m^2 K.

The calculated R-values range from 0.626 to 0.418 W^{-1} m^2 K, corresponding to U-values between 1.598 and 2.392 W m^{-2} K^{-1}. The thermal mass per unit area of the bricks in the wall was estimated as 403,200 J m^{-2} K^{-1}, using a typical brick density of 1600 kg m^{-3} and specific heat capacity of 840 J kg^{-1} K^{-1} [14]. Using a typical density of gypsum of 1440 kg m^{-3} and a specific heat capacity of 840 J kg^{-1} K^{-1} [14] gives a thermal mass per unit area of 12,096 J m^{-2} K^{-1}. The total thermal mass per unit area of the wall is therefore in the region of 415,296 J m^{-2} K^{-1}.

3.1.2. Direct computation: the average method

The average method [22] is a direct computation to estimate the wall's R-value. It assumes steady state heat flow where thermal mass is neglected, as in Eq. (1):

$$R = \sum (T_{int} - T_{ext}) / \sum Q \tag{1}$$

The duration of the measurement campaign, over which the sums are performed, must ensure that thermal mass effects are, on average, zero. Fluctuations in the internal and external air temperatures during and immediately prior to the test will influence the survey length. ISO 9869 [22] states that surveys can last from a minimum of three days to more than seven days. However, monitoring periods of around two weeks are commonly used to achieve satisfactory results [13,23]; for heavyweight constructions, such as masonry walls, longer periods may be used. Changes to the direction of heat flow violate the assumption of steady-state behaviour and analysis of periods when such behaviour is likely, such as the summer, is not possible with the average method. Measurement is generally undertaken during periods with a difference between internal and external temperatures of equal or greater than 10 °C to decrease the impact of error on the results [16]; therefore the average method is typically only used during the winter heating season.

3.2. Building simulation model

3.2.1. Thermal models of the wall

A model of the heat flow is required to apply Bayesian techniques to analyse the in-situ thermal measurements to estimate the thermal properties of a wall. A unique set of model parameters that provide best fit to the heat flux data are determined, assuming that the model is a good description of all the physical processes taking place. An analysis of two models is presented in this paper: a no thermal mass model and a single thermal mass model to allow for a comparison between a model incorporating the average methodology and a model incorporating a thermal mass.

3.2.1.1. The no thermal mass (NTM) model.
The average method of calculating the thermal resistance assumes that over a sufficiently long period the thermal mass in the wall has no impact on total heat flow [22]. A simple model of heat flow through a wall incorporating this assumption was developed, the "no thermal mass" (NTM) model, where a homogeneous heat flow through the wall results from instantaneous changes in temperature. The predicted
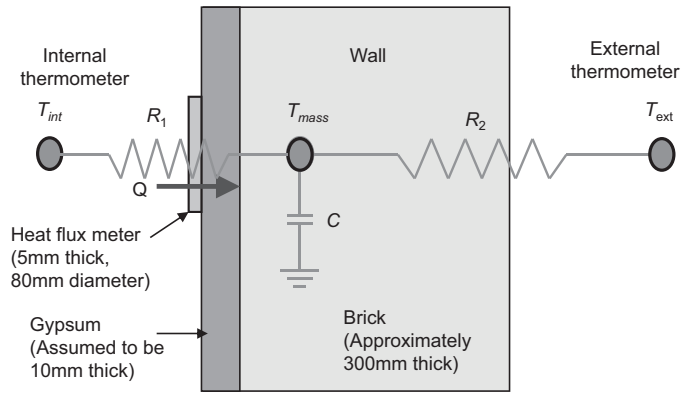

Fig. 1. Schematic diagram, not to scale, showing the electrical equivalent circuit for heat transfer through the wall for the STM model and the arrangement of the thermometers and heat flux plate.

heat flux per unit area (Q) entering the wall at any given time is the difference in the internal (T_{int}) and external (T_{ext}) temperatures divided by the thermal resistance parameter, the R-value (R):

$$Q = (T_{int} - T_{ext}) / R \tag{2}$$

The NTM model has one unknown parameter, R; estimated R-values can be substituted into Eq. (2) and combined with temperature measurements to predict the heat flux flowing through the wall.

3.2.1.2. The single thermal mass (STM) model.
The single thermal mass (STM) model represents the heat flow from the room to the exterior through a wall containing a lumped thermal mass as illustrated by Fig. 1. Heat may be stored or released from the thermal mass creating a time shift and a change in amplitude of the response of the predicted heat flux.

The STM model incorporates four unknown constant parameters:

- the unit area thermal resistance between the internal air and the thermal mass (R_1);
- the unit area thermal resistance between the thermal mass and the external air (R_2);
- the magnitude of the thermal mass per unit area (C);
- the temperature of the thermal mass at the start of the measurements ($T_{mass}^{initial}$).

The constant *instantaneous* heat flow (Q^p) from the internal air to the thermal mass *during* one time step p is calculated using the steady state heat flow equation:

$$Q^p = \left(T_{int}^p - T_{mass}^p\right) / R_1 \tag{3}$$

The temperature of the thermal mass (T_{mass}^p) is initialized to $T_{mass}^{initial}$. The duration of each time step (τ) is the time difference between readings of the data logger, which for the case study data is 5 min. In order to calculate the heat flow in the next time step ($p+1$), the heat flow balance forward-difference equation is used [14]:

$$C \frac{T_{mass}^{p+1} - T_{mass}^p}{\tau} = \frac{T_{int}^{p+1} - T_{mass}^{p+1}}{R_1} + \frac{T_{ext}^{p+1} - T_{mass}^{p+1}}{R_2} \tag{4}$$

Rearranging Eq. (4):

$$T_{mass}^{p+1} = \frac{\frac{T_{int}^{p+1}}{R_1} + \frac{T_{ext}^{p+1}}{R_2} + C \frac{T_{mass}^p}{\tau}}{\frac{1}{R_1} + \frac{1}{R_2} + \frac{C}{\tau}} \tag{5}$$

For any set of parameters R_1, R_2, C and $T_{mass}^{initial}$, combined with time series data for the internal and external air temperatures, the heat entering the wall surface time series can be predicted by repeatedly applying Eqs. (3) and (5).

3.2.2. Estimation of the thermal parameters using Bayesian analysis

3.2.2.1. Bayesian analysis for parameter prediction and model selection. Bayesian analysis was used to estimate the most likely value for the unknown NTM model parameter (R) and of the combination of unknown STM model parameters $(R_1, R_2, C, T_{mass}^{initial})$.

Bayes' theorem [30] states that:

$$p(H_i|D, I) = \frac{p(D|H_i, I)p(H_i|I)}{p(D|I)} \tag{6}$$

where $p(H_i|D,I)$ is the posterior probability, the probability distribution over the parameters of the hypothesis (H_i) given the observed data (D) and any previous knowledge about the wall (I); $p(D|H_i,I)$ is the likelihood function, the parameter probability distribution of obtaining data (D) given the hypothesis (H_i); and $p(H_i|I)$ is the parameter prior probability distribution of the hypothesis. The selection of prior probability distributions of parameters is discussed in Section 3.2.2.2. $p(D|I)$ is the evidence, which is a normalisation factor that is independent of the hypothesis. In the analysis presented in this paper the hypotheses (H_i) and their parameters are either NTM(R) or STM$(R_1, R_2, C, T_{mass}^{initial})$.

The likelihood distribution was calculated using the actual heat flux measurements and the model predictions assuming Gaussian errors. Bayes' theorem was then used to calculate the posterior probability distribution by multiplying the prior probability with the likelihood distributions. The posterior probability distributions for both models were explored using the CERN MINUIT software package [31], which minimises a chi-squared function to find the maximum of a distribution over the multi-dimensional surface of its parameter space. The position maximum of the posterior gives best estimates of the parameters values, whilst the error matrix can be calculated from the covariance matrix.

Bayesian hypothesis testing [30] between the NTM and STM models was undertaken using the odds ratio, which uses the prior distributions, the maximum of the posterior distribution and the error matrix to calculate the ratio of the probability of obtaining the measured data for each model.

3.2.2.2. Prior probability distributions. The prior knowledge of parameters in the NTM and STM models is limited. Ranges of typical thermal resistance and thermal mass for brick built solid walls were calculated in Section 3.1.1. However, the structure and materials comprising the walls monitored in the BSRIA study were identified by visual inspection and not confirmed through measurement [21]. Therefore flat, non-informative prior probability distributions, over a wide range of reasonable values have been adopted to account for our relative ignorance of the thermal properties of the wall:

- the unit area thermal resistances, R (from NTM), R_1 and R_2 (from STM), are greater than zero and less than an arbitrary large value of $3.0\,\mathrm{W}^{-1}\,\mathrm{m}^2\,\mathrm{K}$, more than 4 times the calculated value from Section 3.1.1;
- the effective thermal mass per unit area (C) is greater than zero and less than an arbitrary large value of $2{,}000{,}000\,\mathrm{J\,m}^{-2}\,\mathrm{K}^{-1}$, more than 4 times the expected total thermal mass value from Section 3.1.1;
- the initial temperature of the thermal mass $(T_{mass}^{initial})$ is greater than $-5\,°\mathrm{C}$ and less than $30.0\,°\mathrm{C}$. This range exceeds the lowest observed external temperatures and highest internal temperatures, as illustrated by Fig. 5.

4. Results and discussion

### 4.1. R-value (and U-value) estimation and evolution

An R-value of $0.862 \pm 0.001^{stat}\,\mathrm{W}^{-1}\,\mathrm{m}^2\,\mathrm{K}$ was estimated using the NTM model over the monitoring period and includes a correction for the HFM thermal resistance ($0.000625\,\mathrm{m}^2\,\mathrm{KW}^{-1}$ [28]), only statistical error is shown, error from other sources is discussed in Section 4.2. The corresponding wall U-value is $1.161 \pm 0.001^{stat}\,\mathrm{W\,m}^{-2}\,\mathrm{K}^{-1}$, the average method estimate is also $1.16 \pm 0.06\,\mathrm{W\,m}^{-2}\,\mathrm{K}^{-1}$. The four parameters for the STM model and statistical errors were estimated to be:

- $R_1 = 0.228 \pm 0.001^{stat}\,\mathrm{m}^2\,\mathrm{KW}^{-1}$
- $R_2 = 0.640 \pm 0.001^{stat}\,\mathrm{m}^2\,\mathrm{KW}^{-1}$
- $C = 224{,}256 \pm 2{,}500^{stat}\,\mathrm{J\,m}^{-2}\,\mathrm{K}^{-1}$
- $T_{mass}^{initial} = 12.17 \pm 0.03^{stat}\,°\mathrm{C}$

Combining R_1 and R_2 and subtracting the thermal resistance of the HFM gives a total R-value of $0.867 \pm 0.002^{stat}\,\mathrm{m}^2\,\mathrm{KW}^{-1}$, equivalent to a U-value of $1.153 \pm 0.002^{stat}\,\mathrm{W\,m}^{-2}\,\mathrm{K}^{-1}$. As expected the long term R- and U-values estimated through the NTM and STM models are similar, although outside the statistical error as they represent different physical models (without and with thermal mass). The statistical error is small as it represents the error in the estimation of the parameters that best fit a large amount of data, recorded every 5 min over a 14 day period.

4.2. Evolution of U-values and systematic errors

Fig. 2 shows the evolution of the U-value over time for the NTM and STM models, as the amount of data collected and used in the calculation increases. U-value estimates using the NTM model oscillate on a daily basis, responding to the diurnal temperature changes, whereas the STM model produces more stable U-value estimates. Stability in U-value estimates may be achieved once the effects of thermal mass have been either accounted for directly (STM) or indirectly through averaging (NTM). Using the BSRIA method [21] of taking the point at which U-values vary by less than 1% over a 24 h period as a simple measure of model stability, the STM model achieves stability after 3 days, compared to 10 days for the NTM model (Fig. 2). This definition of stability does not account
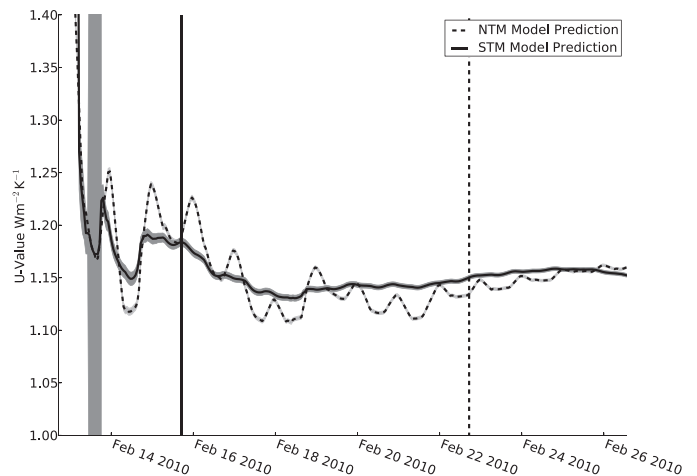
Fig. 2. The evolution of estimated U-values as a function of the amount of data used for the NTM model (dashed line) and the STM model (solid line). The magnitude of the statistical error is also shown as a shaded band around each line. This error reduces to very small values after a very short period of time. The vertical lines indicate the first time that the previous 24 h of U-values are within $\pm 1\%$ of the present U-value: 10 days for the NTM model and 3 days for the STM model.
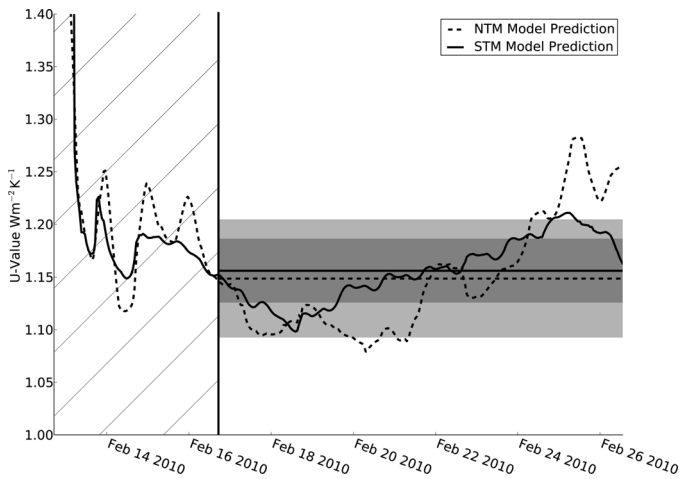
Fig. 3. Plot of the U-value calculated using just the previous 4 days of measurements. The hatched area indicates the running in period of 4 days. The dashed and solid curves represent the running 4 day U-value for the NTM and STM models respectively. The error on the running U-value for both models is very small, only just wider than the thickness of the curves and is therefore not shown. The light grey band with the dashed horizontal line represent the standard deviation and mean of U-values for the NTM model and the dark grey band and solid horizontal line represents the standard deviation and mean of the U-values for the STM model.

for other physical effects that may cause changes to the estimated U-values over different timescales, such as changes to the wind blowing across the wall [32], the influence of air movement due to heating or ventilation systems or to the moisture content of the wall constituent materials [33]. The technique developed here may be used to investigate the impact of such physical issues on U-values.

Fig. 3 shows the variation of U-values estimated from 4 day rolling periods, a timespan over which the diurnal thermal mass effects should be adequately characterised by the STM model. U-values estimated from both the NTM and STM models vary across the measurement period, with a mean and standard deviation of $1.149 \pm 0.056^{stat}\,\mathrm{W\,m^{-2}\,K^{-1}}$ and $1.156 \pm 0.030^{stat}\,\mathrm{W\,m^{-2}\,K^{-1}}$ respectively. Interpreting deviations in U-value as the effect of thermal mass plus physical changes such as variations in wind and moisture, the systematic errors associated with U-value estimation may be estimated.

If deviations in the NTM model result from thermal mass effects in addition to physical changes such as wind and moisture (σ_{W+TM}), whilst deviations in the STM model only result from physical changes (σ_W), the contributions from thermal mass effects may be determined. Assuming statistical independence, thermal mass deviation (σ_{TM}) is estimated ($\sigma_{TM} = \sqrt{\sigma_{W+TM}^2 - \sigma_W^2}$) to be $0.047\,\mathrm{W\,m^{-2}\,K^{-1}}$, larger than the deviation due to physical changes (primarily wind and moisture) of $0.030\,\mathrm{W\,m^{-2}\,K^{-1}}$. The effect of thermal mass on the NTM model may be reduced to less than 1% by recording data for longer than 10 days.

Instrumentation error is estimated from the accuracy of the HFM measurements ($\pm 5\%$ [28]), and the resolution of the thermometer measurements ($\pm 0.1\,^\circ\mathrm{C}$ [27]) to be $\pm 0.051\,\mathrm{W\,m^{-2}\,K^{-1}}$. Combining error estimates, the most likely U-value for the NTM model after the 14 day measurement period U-value is $1.161 \pm 0.001^{stat} \pm 0.030^{sys\text{-}W} \pm 0.051^{sys\text{-}inst} = 1.16 \pm 0.06^{sys+stat}\,\mathrm{W\,m^{-2}\,K^{-1}}$, whilst that for the STM model after the 14 day measurement period U-value is $1.153 \pm 0.002^{stat} \pm 0.030^{sys\text{-}W} \pm 0.051^{sys\text{-}inst} = 1.15 \pm 0.06^{sys+stat}\,\mathrm{W\,m^{-2}\,K^{-1}}$. There are a number of other potential sources of systematic error that are not quantified in these error estimates. These include non-one-dimensional heat flow, radiation effects on thermometers and heat flux meters, very long term changes in wall moisture content and temperature

dependant changes in the thermal properties of the wall. This list is not exhaustive.

4.3. Comparison of U-values estimates

Calculated U-values based on assumed properties of the wall studied range from 1.598 to $2.392\,\mathrm{W\,m^{-2}\,K^{-1}}$ (Section 3.1.1), whereas those estimated by the average method, NTM and STM models are $1.16 \pm 0.06\,\mathrm{W\,m^{-2}\,K^{-1}}$, $1.16 \pm 0.06^{sys+stat}\,\mathrm{W\,m^{-2}\,K^{-1}}$ and $1.15 \pm 0.06^{sys+stat}\,\mathrm{W\,m^{-2}\,K^{-1}}$ respectively. In-situ measurements suggest that the thermal performance of the wall is significantly better (>37%) than revealed by simple calculations, which could be caused by differences in wall structure or material properties, neither of which may be identified by visual inspection. The STM analysis method was used for all the walls in the BSRIA sample showing a similar difference between U-values estimated from simple calculations and in-situ measurements. The predicted energy and cost savings associated with interventions in this property, such as retrofitting with solid wall insulation, could be significantly over-estimated by the use of the simple calculation leading to a longer than expected payback period. We are currently analysing the full sample of 93 properties to investigate these issues further.

4.4. Dynamic performance of models

U-value estimates for the NTM and STM models are very similar after all the data from the full 14 day measurement period are used. However, Fig. 4 highlights the large differences in dynamic heat flow predicted by the two models. The NTM model does not describe the heat flux data well, having a standard deviation of the residuals (i.e. differences between the model prediction and measurement) of $4.5\,\mathrm{W\,m^{-2}}$. The STM model describes the dynamic heat flow much better than the NTM model, with a standard deviation of residuals of $0.9\,\mathrm{W\,m^{-2}}$.

Eq. (6) shows that taking the ratio of the posterior probabilities, $p(H_i|D,I)$ (the probability that the hypothesis (H_i) is true, given the observed data (D)) obtained through applying different hypotheses (models), the ratio of the probability of those models accurately describing the observed data may be obtained. This ratio, the odds ratio, embodies Occam's razor and may be used to select the model with the greatest likelihood of describing the observed data [30]. The odds ratio for the ability of the STM compared to the NTM
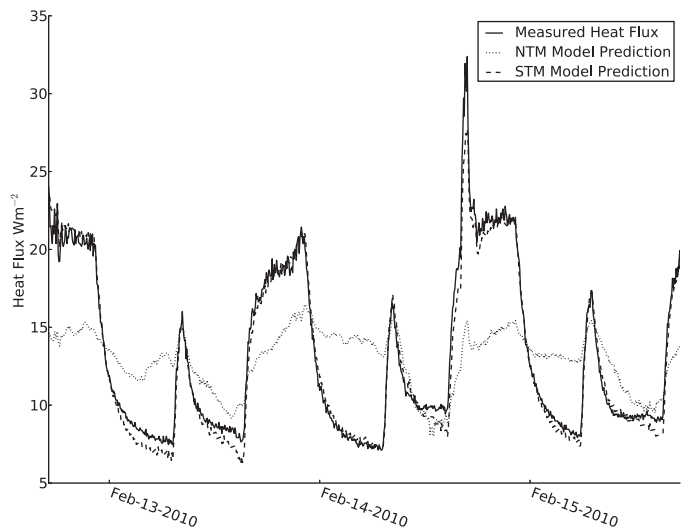
Fig. 4. Measured (solid line) and predicted heat flux using NTM model (dotted line) and STM model (dashed line). A reduced time period is shown for clarity.
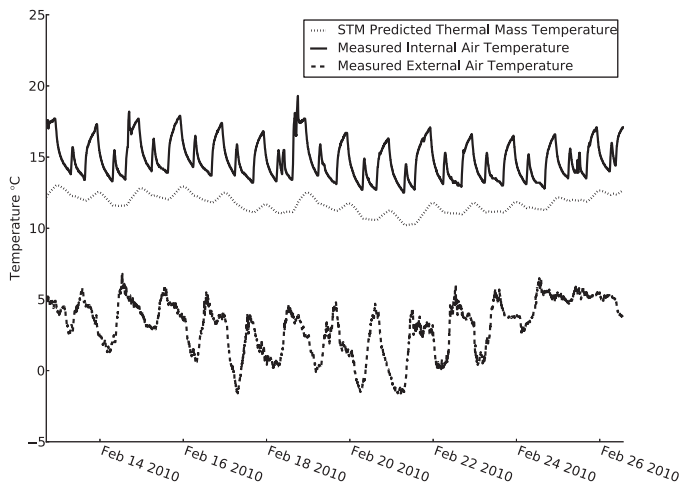
Fig. 5. Measured internal (solid line) and external (dashed line) air temperatures. Estimated thermal mass temperature predicted by the STM model is shown by the dotted line.

model to describe the heat flux and temperature data is extremely large ($10^{2,757}$) and is partly attributable to the large number of data points analysed. Therefore, we can be certain that the STM model better characterises the heat flux data than the NTM model, owing to the addition of the thermal mass.

4.5. Wall structure and thermal mass

The STM model, whilst describing the heat flux data well, is a greatly simplified model from the physical construction and environment of the actual wall, and subsequently the heat flow through it. The STM model aggregates the effective thermal mass into a single point source component, as illustrated by Fig. 1, rather than the continuum of thermal mass in a real wall. Application of the STM model therefore yields an effective thermal mass which, in combination with the resistances, best describes the heat flux and temperature data for a heat flux meter placed on the inside surface of the wall. The thermal mass per unit area estimated through the STM model is $224{,}000 \pm 19{,}000^{\text{sys-stat}}\,\text{J}\,\text{m}^{-2}\,\text{K}^{-1}$. As expected it is significantly lower than that estimated using the thermal properties of the constituent components of the wall ($415{,}296\,\text{J}\,\text{m}^{-2}\,\text{K}^{-1}$, Section 4.1.1). Fig. 5 shows the predicted thermal mass temperatures: they are closer in magnitude to internal temperatures and oscillate diurnally and, as expected, are out of phase with both internal and external temperatures. The properties of the effective thermal mass were further investigated by using R_1 and R_2 to estimate the location of the thermal mass as a fraction of the total resistance of the wall. The unit thermal resistances from the STM model $R_1 = 0.228\,\text{W}^{-1}\,\text{m}^2\,\text{K}$, $R_2 = 0.640\,\text{W}^{-1}\,\text{m}^2\,\text{K}$ and the unit internal and external surface resistances 0.13 and $0.04\,\text{W}^{-1}\,\text{m}^2\,\text{K}$ [14] respectively, were used. Assuming a homogeneous wall 300 mm wide, the effective thermal mass per unit area is only 40 mm from the internal surface of the wall (14% of the total thickness of the wall). This highlights that the dynamic internal thermal performance of buildings is dominated by thermal masses closely coupled to the interior air, in addition to sources and sinks of heat, and not to the whole thermal mass of adjacent materials.

5. Conclusions

A new technique for significantly reducing the monitoring period required to estimate the thermal properties of building elements using in-situ measurements has been presented and compared to the conventional steady-state in-situ method and values

calculated using assumed material properties for a case study wall. Simple physical models of the building element, based on electrical analogy, are combined with Bayesian analysis. The technique may be used to estimate thermal properties, including error estimates, and to compare the probability that different models may have produced the observed data. Two simple models of the wall have been compared: a single thermal resistance, no thermal mass model (NTM) and a two thermal resistance, single thermal mass model (STM). Further models of the wall could be tested, but the STM model is the most complex that can be used to find unique solutions for the parameters without the addition of extra monitoring equipment.

The conventional averaging method of estimating U-values from 14 days of in-situ measurements of heat flux, internal and external temperatures gives $1.16 \pm 0.06\,\text{W}\,\text{m}^{-2}\,\text{K}^{-1}$, the same as the equivalent NTM model and Bayesian estimation of the U-value: $1.16 \pm 0.06^{\text{sys+stat}}\,\text{W}\,\text{m}^{-2}\,\text{K}^{-1}$. The U-value estimated from the STM model ($1.15 \pm 0.06^{\text{sys+stat}}\,\text{W}\,\text{m}^{-2}\,\text{K}^{-1}$) is very similar to that from the NTM model; values incorporate estimates of systematic errors. As expected, the averaging method, the NTM and STM models give similar results for all 93 walls measured during the BSRIA trials [21].

The STM model accounts for the impact of thermal mass on estimated U-values after three days, compared to 10 days for the NTM model: a significant reduction to the time required to thermally characterise the wall. However, estimated U-values continued to evolve after the values were first stable to within ±1% over 24 h. The impact of changing heat transfer due to environmental factors, such as changes to the wind or moisture, were investigated by calculating rolling 4 day U-values with the STM model. Uncertainty due to varying environmental conditions was estimated from the standard deviation of these rolling U-values and is the largest contribution to total error; extended monitoring periods may be used to characterise the performance of building elements accounting for changes in environmental factors. The relatively short timescale required to estimate U- and R-values using this technique makes it well suited to investigating their potentially significant dependence on environmental factors such as wind speed [32].

The STM model was able to reproduce the time evolving heat flux entering the wall from the room more accurately than the NTM model. The probability that the NTM and STM models accurately describe this dynamic data was estimated through the Bayesian Occam's factor, providing very strong evidence supporting the inclusion of thermal mass in the STM model. The effective thermal mass per unit area of the wall was estimated to be $224{,}000 \pm 19{,}000^{\text{sys-stat}}\,\text{J}\,\text{m}^{-2}\,\text{K}^{-1}$, compared to that calculated from published values of approximately $412{,}000\,\text{J}\,\text{m}^{-2}\,\text{K}^{-1}$. The estimated effective thermal mass of the wall is just 40 mm from the interior wall surface in this 300 mm thick wall and represents the apparent thermal mass of the wall from the perspective of the interior space.

The method presented here, combining physical models and Bayesian analysis can be used to significantly reduce the monitoring period required to estimate U- and R-values, compared to conventional steady-state methods. The method utilises dynamic changes in temperature, rather than requiring a consistently high temperature difference (as for steady state methods). This feature may be used to analyse in-situ measurements taken in summer, albeit with higher uncertainty in results due to a greater influence of potential systematic errors.

Accurate knowledge of the thermal properties of building elements is essential to inform the decision making processes at all levels, when estimating the energy savings and cost effectiveness of retrofit measures, such as installing insulation. However, a performance gap has been identified in the cost-effectiveness and energy savings of interventions, based on their expected U-values [34] and is illustrated by the walls analysed here which exhibited

significantly lower than expected U-values (expected range from 1.6 to $2.4\,\mathrm{W\,m^{-2}\,K^{-1}}$, vs measured $1.15\pm0.06^{sys+stat}\,\mathrm{W\,m^{-2}\,K^{-1}}$ for the STM model). The U- and R-value estimation technique presented may be used to significantly shorten the monitoring period required per building element, enabling more cases to be cost-effectively measured and promoting better informed decision making. The short timescale of this technique is also well suited to investigating the impact of weather on U-values and the estimation of effective thermal mass may inform thermal comfort considerations.

Acknowledgements

References

[1] International Energy Agency, 2011. Technology Roadmap. Energy-efficient Buildings: Heating and Cooling Equipment. OECD/IEA, Paris (F).

[2] European Commission for Climate Actions, 2009. The EU Climate and Energy Package [online]. [Accessed 10th October 2013]. Available from: http://ec.europa.eu/clima/policies/package/documentation_en.htm

[3] European Commission for Climate Actions, 2011. Communication from the commission to the European Parliament, the Council, the European Economic and Social Committee and the Committee of Regions. A Roadmap for moving to a competitive low carbon economy in 2050.

[4] Climate Change Act 2008, Part 1, United Kingdom: Department of Energy and Climate Change.

[5] D.B. Crawley, J.W. Hand, M. Kummert, B.T. Griffith, Contrasting the capabilities of building energy performance simulation programs, Building and Environment 43 (2008) 661–673.

[6] L.G. Swan, V.I. Ugursal, Modeling of end-use energy consumption in the residential sector: a review of modeling techniques, Renewable and Sustainable Energy Reviews 13 (2009) 1819–1835.

[7] Building Research Establishment. 2011. The Government's Standard Assessment Procedure for Energy Rating of Dwellings. 2009 Edition, Garston, Watford (UK): BRE.

[8] ISO 13790, 2008. Energy performance of buildings – calculation of energy use for space heating and cooling.

[9] European Parliament and Council. 2010. Directive 2010/31/EU: Energy Performance of Buildings.

[10] J.R. Stein, A. Meier, Accuracy of home energy rating systems, Energy 25 (2000) 339–354.

[11] S.H. Hong, T. Oreszczyn, I. Ridley, The impact of energy efficient refurbishment on the space heating fuel consumption in English dwellings, Energy and Buildings 38 (2006) 1171–1181.

[12] S. de Wit, Uncertainty in building simulation, in: A. Malkawi, G. Augenbroe (Eds.), Advanced Building Simulation, Taylor & Francis, Abingdon (UK), 2004.

[13] C. Rye, C. Scott, U-Value Report (The SPAB research report 1), 2012 Edition, The Society for the Protection of Ancient Buildings (SPAB), London (UK), 2011.

[14] J.P. Holman, Heat Transfer, Ninth Edition, McGraw- Hill, 2002.

[15] P.G. Cesaratto, M. De Carli, A measuring campaign of thermal conductance in situ and possible impacts on net energy demand in buildings, Energy and Buildings 59 (2013) 29–36.

[16] A. Byrne, G. Byrne, A. Davies, A.J. Robinson, Transient and quasi-steady thermal behaviour of a building envelope due to retrofitted cavity wall and ceiling insulation, Energy and Buildings 61 (2013) 356–365.

[17] B.R. Anderson, Site-Testing Thermal Performance: a CIB survey. Batiment International, Building Research and Practice 12 (1984) 147–149.

[18] J.B. Siviour, Experimental U-values of some house walls, Building Services Engineering Research and Technology 15 (1) (1994) 35–36.

[19] A.W. Pratt, Heat Transmission in Buildings, John Wiley and Sons, 1981.

[20] EN ISO 13786. 2007. Thermal performance of building components–Dynamic thermal characteristics–Calculation methods.

[21] S. Birchall, C. Pearson, R. Brown, Solid Wall Insulation Field Trial – Baseline Performance of the Property Sample. Report 53588/x, BSRIA Limited, Bracknell (UK), 2011.

[22] ISO 9869.1994. Thermal insulation–Building Elements–In-situ measurement of thermal resistance and thermal transmittance.

[23] Energy Saving Trust. 2005. GIR 64: Post-construction testing–a professional's guide to testing housing for energy efficiency (2005 edition).

[24] P.H. Baker, H.A.L. van Dijk, PASLINK and dynamic outdoor testing of building components, Building and Environment 43 (2008) 143–151.

[25] O. Gutschker, Parameter identification with the software package LORD, Building and Environment 43 (2008) 163–169.

[26] M.J. Jimenez, B. Porcar, M.R. Heras, Application of different dynamic analysis approaches to the estimation of the building component U value, Building and Environment 44 (2009) 361–367.

[27] Eltek. 2013. Squirrel 450/850 Series Data Logger. [Accessed October 2013]. Available at: http://www.eltekdataloggers.co.uk/450_logger.shtml

[28] Hukseflux. 2013. HFP01 Product Brochure, version 1003. [Accessed on October 2013]. Available at: http://www.hukseflux.com/sites/default/files/product_brochure/HFP01 v1003.pdf

[29] Baker, P. 2011. Historic Scotland Technical Paper 10–U-values and traditional buildings. In situ measurements and their comparisons to calculated values. [Accessed October 2013]. Available at: http://www.historic-scotland.gov.uk/technicalpapers

[30] P. Gregory, Bayesian logical data analysis for the physical sciences, 10, Cambridge University Press, Cambridge (UK), 2005.

[31] James, F. and Winkler, M. 2004. MINUIT User's Guide [online]. Geneva (CH): Organisation Européen pour la Recherche Nucléaire (CERN). [Accessed on September 2013]. Available at: http://seal.web.cern.ch/seal/documents/minuit/mnusersguide.pdf

[32] Bankvall, C.G. 1977. Påtvingad konvektion. Praktisk värmeisoleringsförmåga under inverkan av vind och arbetsudförande, (Forced Convection. Thermal Insulation influenced by wind and workmanship). Report 1977:21, Stockholm (S): Statens Provningsanstalt.

[33] H.M. Künzel, Simultaneous heat and moisture transport in building components one- and two-dimensional calculation using simple parameters, IRB Verlag (1995) 1995.

[34] Doran, S. 2000. Field investigations of the thermal performance (U-values) of construction elements–as built. BRE Report 78132, Watford (UK): BRE.